

Majorana zero modes are the edge modes?

Vijay Pathak,^{*} Vaishnav Mallya, and Sujit Sarkar[†]

Theoretical Sciences Department, Poornaprajna Institute of Scientific Research, Bengaluru, India 562 164

(Dated: June 26, 2025)

Topological phases are typically characterised by a topological invariant: winding number, which indicates the number of zero modes expected in a given phase. However, the winding number alone does not capture the qualitative differences between the modes within the same topological phase. In this work, we present an analytical solution for the zero-energy modes across various regimes of the phase diagram; a result that, to our knowledge, has not been reported previously in the literature. Through this solution, we characterise edge modes coexisting in a single phase and systematically classify them based on their spatial behaviour. Our analysis also identifies parameter regions where one or both zero modes are perfectly localised at the system edges. Finite and infinite systems were compared based on their spatial characteristics of zero modes. In addition, we provide a detailed analytical treatment of the characteristic equation, demonstrating that its roots offer further insight into the nature of the topological phase transitions. The whole study is based on a one-dimensional quantum Ising chain with long range interactions.

I. INTRODUCTION

Majorana zero modes (MZMs) [1–4] have become a huge topic of interest in recent years, have been experimentally realised [5], as topological quantum computers are being seen as a candidate that can be used to realise fault-tolerant quantum computation [5], [6], where MZMs are zero energy modes with Majorana properties. Majorana operators are self-conjugate and commute with the Hamiltonian. Through his seminal paper [7], A. Y. Kitaev proposed a model for topological superconductors and explained how Majorana quasiparticles hosted at the edges of the topological chain can be used to construct qubits that are protected from local perturbations naturally because of the non-local nature of qubits and topological protection [8]. This shields the qubits from decoherence, one of the main challenges in building scalable quantum computers.

A key concept for hosting Majorana zero modes in the presence of distinct topological phases defined by the global topological invariant, winding number (w). A phase transition occurs when the energy gap closes and then reopens, where the closing of the gap signifies the critical point for the transition. By keeping the system the same but subjecting it to an open boundary, bulk-boundary correspondence separates the boundary modes distinctly from the bulk modes. It is demonstrated that the number of boundary modes is the same as the winding number in a specific phase [9]. As long as the energy gap is open, the change in the system's parameters within the phase will not change w and the number of boundary modes. Introducing higher orders of interactions opens to new topological phases and higher winding numbers, increasing the number of possible MZMs hosted in the chain [10].

One of the model systems used to extensively study MZMs is the 1D Kitaev chain. The quantum Ising is a special case of the Kitaev model with hopping and pairing terms equal. In this work, we consider the quantum Ising model with nearest- and next-nearest-neighbour interactions [11, 12], which offers a richer platform [13] for analytically investigating the behaviour of edge modes across different topological phases [9]. The quantum Ising model, after being subject to the Jordan-Wigner transformation, is mapped to a system of spinless fermions. To further probe the properties of the edge modes, the fermionic Hamiltonian is expressed in the Majorana bases, where each real fermion is decomposed into two complex Majorana operators. The transformation reveals the intrinsic particle-hole symmetry of the system and explicitly brings MZMs into view. These bases also help in finding the parameter domain of different phases. Moreover, the Majorana basis transformation enables the derivation of the recursion relation for the zero-mode profile, as well as a clear distinction between topologically trivial and non-trivial phases and also between different topological phases. These properties lay the foundation of our analysis presented in this work.

Our main focus is to understand the difference between zero, edge, and Majorana modes. To gain a deeper understanding of how the system supports MZMs, we systematically examine their behaviour under varying parameters and system sizes. We uncovered several notable features of the edge modes, including their types, spatial profiles, and conditions under which they exhibit different decay modes. We posed the question of whether zero modes preferentially localise at specific sites, and what determines this behaviour. We characterise the zero modes, along with their

^{*} vijay@ppisr.res.in

[†] sujit.tifr@gmail.com

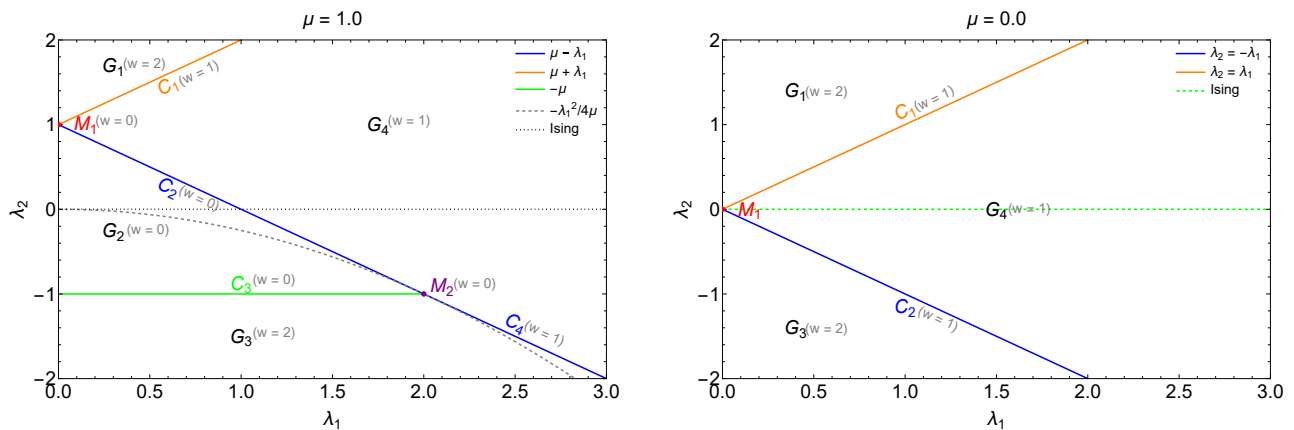


FIG. 1: (Color online) Phase diagram with different regimes. The left figure is for $\mu = 1$ and the right is for $\mu = 0$. It can be noticed here that the $w = 0$ region (G_2), the critical line C_3 and the dashed curve are absent from the $\mu = 0$ phase diagram.

analytical justification, in different topological regimes and parametric conditions to understand what distinguishes one parametric point from another within a single phase. Furthermore, we investigated how MZMs evolve from finite chains [14] to near-infinite chains and demonstrated how energy plays a key role in localisation and overlap of edge modes in a finite-sized chain. While some systems exhibit the edge modes but do not strictly possess zero energy, nor do they fully exhibit Majorana properties, this is due to the finiteness of the chain. These are called massive edge modes [15], [10], and studies have been performed to characterise them extensively.

The paper is structured as follows: Section II walks through the model Hamiltonian utilised, its Nambu spinor form and the phase diagram. Section III shows the basis transformed Hamiltonian and the recursion relation tied to it. The reader is also shown how the roots of the characteristic equation of the recursion relation can characterise a phase transition in this section. Section III B deals with the different types of edge modes and the conditions under which they form. Section IV draws attention towards the finite size effects, while further sections highlight the conclusions. There is an appendix section with more details.

II. MODEL SYSTEM

The Hamiltonian can represent the extended Ising model with next-nearest neighbour interaction [9]

$$H = -\mu \sum_{j=1}^N (1 - 2c_j^\dagger c_j) - \lambda_1 \sum_{j=1}^{N-1} (c_j^\dagger c_{j+1} + c_j^\dagger c_{j+1}^\dagger + h.c) - \lambda_2 \sum_{j=2}^{N-1} (c_{j-1}^\dagger c_{j+1} + c_{j+1}^\dagger c_{j-1}^\dagger + h.c) \quad (1)$$

The parameters μ , λ_1 , and λ_2 are external field, nearest neighbour, and the next-nearest neighbour couplings, respectively.

By imposing periodic boundary conditions, the Hamiltonian can be diagonalized by a Bogoliubov transformation:

$$H = \vec{\chi} \cdot \vec{\sigma} = \chi_z(k) \sigma_z - \chi_y(k) \sigma_y \quad (2)$$

where $\chi_z(k) = -2\lambda_1 \cos k - 2\lambda_2 \cos 2k + 2\mu$ and $\chi_y(k) = 2\lambda_1 \sin k + 2\lambda_2 \sin 2k$. The excitation spectra [9] are

$$\epsilon_k = \pm \sqrt{\chi_y^2(k) + \chi_z^2(k)} \quad (3)$$

The critical lines $\lambda_2 = \mu + \lambda_1$, $\lambda_2 = \mu - \lambda_1$, and $\lambda_2 = -\mu$ are found by making the energy equation zero, so gap closing points can be found (Appendix VI A). Topological quantum phase transitions are where the gap closes. The gap-closing point can depend on the system's parameters. The edge modes are possible in open boundary conditions because the environment around them is different from the bulk, and the Hamiltonian is converted into the $2N \times 2N$

form, $H \equiv \begin{pmatrix} \hat{h} & \hat{\Delta} \\ \hat{\Delta}^\dagger & -\hat{h} \end{pmatrix}$ using Nambu bases $\begin{pmatrix} c \\ c^\dagger \end{pmatrix}$ [16], where the submatrices are given by,

$$\hat{h}_{ij} = -\frac{\lambda_1}{2}(\delta_{j,i+1} + \delta_{j,i-1}) - \frac{\lambda_2}{2}(\delta_{j,i+2} + \delta_{j,i-2}) + \mu\delta_{ij}, \quad (4)$$

$$\hat{\Delta}_{ij} = -\frac{\lambda_1}{2}(\delta_{j,i+1} - \delta_{j,i-1}) - \frac{\lambda_2}{2}(\delta_{j,i+2} - \delta_{j,i-2}). \quad (5)$$

. The eigen vector equation will be as follows

$$\begin{pmatrix} \hat{h} & \hat{\Delta} \\ \hat{\Delta}^\dagger & -\hat{h} \end{pmatrix} \begin{pmatrix} \vec{u}_n \\ \vec{v}_n^* \end{pmatrix} = E_n \begin{pmatrix} \vec{u}_n \\ \vec{v}_n^* \end{pmatrix} \quad (6)$$

The probability at site j is $P_j = |u_j|^2 + |v_j|^2$. If the left and right sides of the chain are not connected, then it is an open boundary. The winding number (w) is calculated from the Anderson pseudo-spin. The winding number can change from one phase to another. The winding number is also shown to be equal to the same number of normalizable MZMs. Phase transition lines select the lower edge modes from the two phases that are joining. The number of normalizable zero modes (w) for different phases is shown in Fig. 1. Since Majorana modes are hermitian, the eigenvectors for zero energy will satisfy the condition $\vec{u} = \vec{v}$ or $\vec{u} = -\vec{v}$ for left and right modes.

III. PHYSICS FROM MAJORANA BASES

If we convert the Fermion bases operators, c and c^\dagger , into the Majorana bases operators, then the Hamiltonian (Eq. 1) will take the following form.

$$H = -2i \left[-\mu \sum_{i=1}^N b_i a_i + \lambda_1 \sum_{i=1}^{N-1} b_i a_{i+1} + \lambda_2 \sum_{i=2}^{N-1} b_{i-1} a_{i+1} \right] \quad (7)$$

where normalised operators $a_i = \frac{c_i^\dagger + c_i}{\sqrt{2}}$ and $b_i = -\frac{i(c_i^\dagger - c_i)}{\sqrt{2}}$ such that $\{a_i, a_j\} = \delta_{i,j}$ and $\{b_i, b_j\} = \delta_{i,j}$ and $\{a_i, b_j\} = 0$.

If the basis for the Hamiltonian is chosen to be $(a_1, b_1, a_2, b_2, \dots, a_N, b_N)$, then the eigenvector associated with the eigenvalue E can be found from the following eigenvector equation in recursive form.

$$-\mu A_j + \lambda_1 A_{j+1} + \lambda_2 A_{j+2} = iE A'_j \quad (8a)$$

$$\mu A'_j - \lambda_1 A'_{j-1} - \lambda_2 A'_{j-2} = iE A_j \quad (8b)$$

with $A_{-1} = 0 = A_{-2}$ and $A_{N+1} = 0 = A_{N+2}$, where eigenvector will be of the form $(A_1, A'_1, A_2, A'_2, \dots, A_N, A'_N)^T$. For $j = 1$, the second equation will be $\mu A'_1 = iE A_1$ and for $j = N$, the first equation will be $-\mu A_N = iE A'_N$. If the energy is exactly zero, $A_N = 0 = A'_1$ even for finite A_1 and A'_N . The recursion relations will make all subsequent A'_j and A_j zero. To find an eigenvector corresponding to zero energy, both equations should be simultaneously satisfied. This creates an inconsistency as it would imply a zero solution for the entire mode and is a consequence of assuming E to be exactly zero. This inconsistency arises directly from the structure of the Hamiltonian, not from any assumption. This issue is not observed experimentally or for the mode directly obtained from the Hamiltonian numerically in a finite chain because the energy is never exactly zero; rather, a very small number is present. This small energy with decaying feature of zero modes can satisfy the equations without any inconsistency because the left (right) mode will have almost zero A_N but not exact zero and A'_N and E are very small so this will not propagate to make A_1 zero and A_j can be finite for left ends of the chain. In the case of an infinite chain, no such boundaries exist to enforce the vanishing of odd terms and vice versa, making the construction of normalizable modes possible. The recursion relation for the zero mode will be

$$-\mu A_j + \lambda_1 A_{j+1} + \lambda_2 A_{j+2} = 0 \quad (9)$$

where the form of the eigenvector will be $(A_1, 0, A_2, 0, \dots, A_N, 0)^T$. If we take an ansatz $A_i = r^i$, then the general solution of the above equation will be

$$A_j = C_1 q_+^j + C_2 q_-^j \quad (10)$$

where, $q_{\pm} = \frac{-\lambda_1 \pm \sqrt{\lambda_1^2 + 4\mu\lambda_2}}{2\lambda_2}$ are the roots of the equation $\lambda_2 q^2 + \lambda_1 q - \mu = 0$. The probability at site j will be $P_j = |A_j|^2$.

Though there is a double degeneracy of zero eigenvalues in Nambu bases, this polynomial gives only half because w tells how many zero modes will be at each chain end. By definition, there should be w modes at either end without any overlap. This ansatz automatically satisfies that condition, but with a cut-off size that depends on the parameters. To find out modes at the right end, the ansatz should be r^{-j} .

The normalizable solutions will be possible if $|q_{\pm}| < 1$. Based on this (Appendix VID), the number of zero modes in different regions is shown in Fig. 1. If both solutions are normalizable, then the general solution can be written in terms of two physically realisable initial conditions, namely the first and second sites' amplitude coefficients, A_1 and A_2 (Appendix VIE)

$$A_j = \frac{1}{q_+ - q_-} [A_1(q_-^{j-1}q_+ - q_-q_+^{j-1}) + A_2(q_+^{j-1} - q_-^{j-1})]$$

This solution is true only if $q_+ \neq q_-$. Any two sets of initial conditions will yield two edge modes, provided they are orthogonal to each other; otherwise, they will be made by an orthogonalisation procedure:

$$\vec{B} = \vec{A}_2 - \frac{\langle \vec{A}_2 | \vec{A}_1 \rangle}{\langle \vec{A}_1 | \vec{A}_1 \rangle} \vec{A}_1$$

Where \vec{A}_1, \vec{A}_2 are two vectors found from two sets of initial conditions. \vec{B} is the orthogonal vector to \vec{A}_1 which satisfies the recursion relation since it is a linear combination of two known solutions. For the $w = 1$ region, the coefficient of $|q| \geq 1$ will be considered zero for the normalised edge solution, so the solution will be

$$A_j = cq^j$$

where q is the normalisable solution out of q_{\pm} . For $w = 0$, both coefficients have to be zero, so no eigenvector.

Although the recursion relation appears independent of size, it is derived from the assumption that the energy is zero, which depends on size. If size is not chosen correctly, then the energy will not be zero, and the relation will not be applicable to find zero modes.

A. Phase transition determined from the roots (q) of the characteristic equation

Since $\lambda_1 \geq 0$, whenever one of the $|q|$ is greater than one, then that will be q_- . All the transition lines and points will have $|q| = 1$ for the unnormalised mode; however, within the regions, it will be greater than one for the unnormalised mode. $|q|$ varies continuously from one region to another, unlike the winding number, which remains constant; therefore, $|q|$ can also serve as an indicator of a phase transition and, in addition, of the distance from the critical points or lines. When it is always real, the variation is smooth (top and middle panels of Fig. 2); however, when it transitions from complex to real, the change is abrupt (bottom panel of Fig. 2). For $\lambda_1^2 + 4\mu\lambda_2 < 0$, $|q| = \sqrt{\frac{-\mu}{\lambda_2}}$ is independent of λ_1 that is why $|q_{\pm}|$ is constant till it meets $\lambda_1^2 + 4\mu\lambda_2 = 0$ point. At this point $\mu = \frac{-\lambda_1^2}{4\lambda_2}$ which

converts $|q \pm| = \sqrt{\frac{\lambda_1^2}{4\lambda_2^2}} = \frac{|\lambda_1|}{2|\lambda_2|}$. The same thing you get directly from $q_{\pm} = \frac{-\lambda_1}{2\lambda_2}$ at the meeting point which also

gives $|q_{\pm}| = \frac{|\lambda_1|}{2|\lambda_2|}$. Similarly, in this region, the transition is continuous but not smooth, unlike the other regions.

The *top panel* image shows that $|q_+|$ is always less than one, but $|q_-|$ increases with increasing λ_1 for fixed λ_2 and μ . When $\lambda_1 < 0.8$ it remains in G_1 region at $\lambda_1 = 0.8$ it is on transition line C_1 , $|q_-| = 1$ and for $\lambda_1 > 0.8$, $|q_-| > 1$ so it enters in G_4 and keeps increasing with λ_1 . The *middle panel* also shows a similar trend, except that till q 's are complex (See dashed part in Fig. 1), both $|q|$ are the same and less than one. After that, $|q_+|$ will keep decreasing, but $|q_-|$ will keep increasing but will be less than one till $\lambda_1 < 2.8$, and at $\lambda_1 = 2.8$, $|q_-| = 1$ and after that it will be higher than one. This trend is because it goes from G_3 to G_4 via the transition line C_4 . The *bottom panel* shows $|q_-|$ is always higher than one and keeps increasing with λ_1 , but $|q_+|$ decreases from higher than one to less than one via a transition point at $\lambda_1 = 0.8$. This is because it goes from G_2 to G_4 .

A similar continuous transition from $|q|$ by varying λ_1 is observed for fixed λ_2 . Though at $\lambda_2 = 0$, which is the conventional quantum Ising case, both $|q_{\pm}|$ appear to be undefined, but q_+ will have $\frac{0}{0}$ form which has a valid limiting

value equals to $\frac{\mu}{\lambda_1}$. The diverging q_- without a limiting value suggests there is only one normalisable zero mode. A similar result can be found from the quantum Ising model with recursion relation $\lambda_1 A_{j+1} = \mu A_j$, which will have the same $|q|$ for the only existing mode.

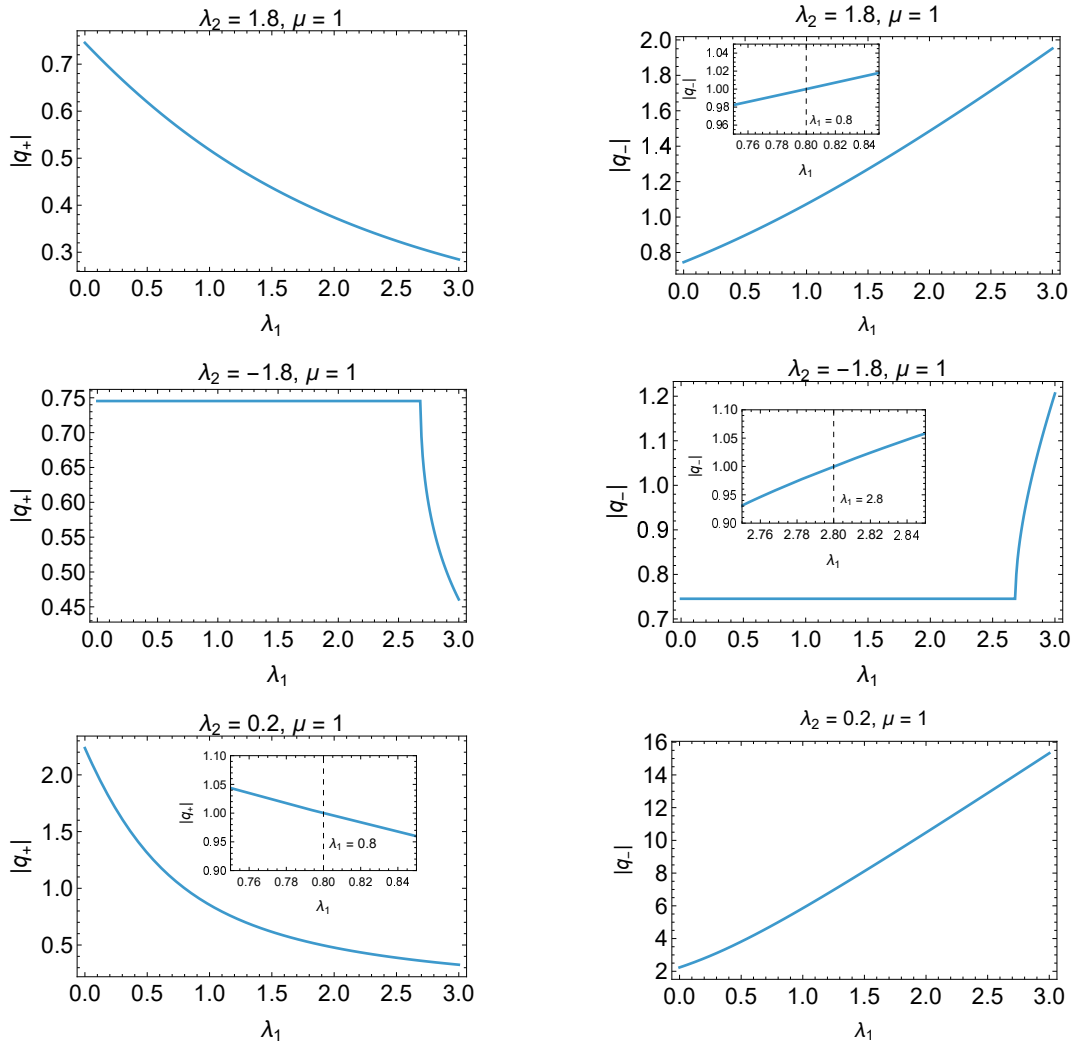


FIG. 2: (Color online) Plots of $|q|$ versus λ_1 shows the phase transition from the region G_1 to region G_4 through critical line C_1 (top), from region G_3 to region G_4 through critical line C_2 (middle), and from region G_2 to region G_4 through critical line C_2 (bottom) in Fig. 1. The dashed line in different insets shows the corresponding critical point.

B. Different types of zero modes

Edge modes are considered to be present whenever the probability is higher at the edge of the chain than in the bulk. This definition works nicely for zero modes whenever there is only one edge mode, but if there are more than one edge mode, then what will be the nature of the second one? A simple case, discussed in detail later, is when there are two perfectly localised modes; they both cannot be on the first site, so that the second one will be on the second site. So, one zero mode is edge mode, but the other one is bulk. There are cases, discussed later, where the highest probability is also located deep within the bulk. There can be different types of zero modes: (a) the left and right overlapping modes. (b) perfectly left- or right modes. (c) perfect left- or right-edge modes and possessing Majorana properties. Within all these categories, the modes can be perfectly decaying, oscillatory decaying, or perfectly localised modes. There are cases when energy is not zero, but it has the highest probability towards the edge and decaying probability towards the bulk. Let us analyse the different cases for parameters within individual phases:

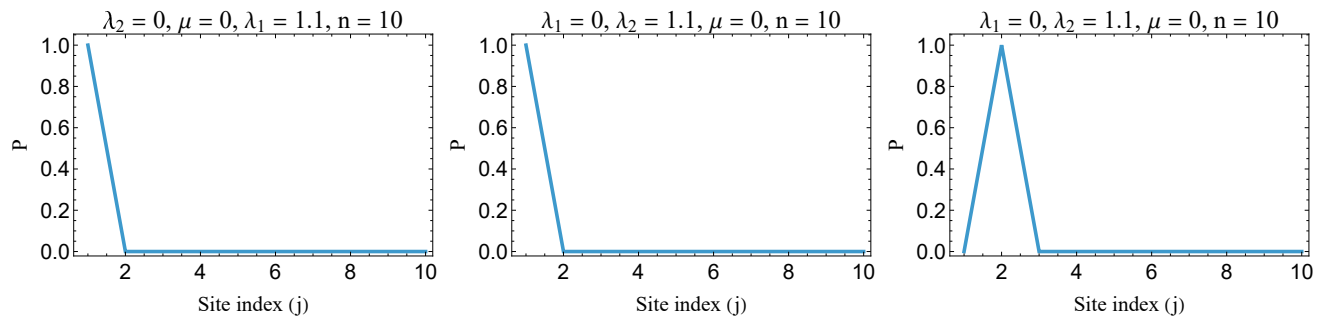


FIG. 3: (Color online) Probability distribution (P) at different sites (j) is plotted. (Left) The single zero mode observed for $\lambda_2 = 0$ and $\mu = 0$. This is the perfect localised mode situated at site one since the probability at all other sites is zero. (Middle and Right) There are two zero modes when $\mu = 0, \lambda_1 = 0$. These two modes are also perfectly localised modes situated at the first and second sites, respectively. All of them have exact zero energies.

1. $\mu \neq 0, \lambda_1 = 0, \lambda_2 = 0$

This parameter space is a trivial case of the conventional quantum Ising model where only a chemical potential is present. This will keep all lattice sites disconnected from each other because pairing terms are zero. The recursion relation for the case will be $\mu A_j = 0$, which asks for all A_j to be zero if zero energy is present; that is why there is no zero energy in the open boundary. This case lies at the $(0, 0)$ point in the region G_2 in the left Fig. 1

2. $\mu = 0, \lambda_1 \neq 0, \lambda_2 = 0$

This is a special case of the quantum Ising model. In the phase diagram for $\mu = 0$ (right figure of Fig. 1), this case is represented by a green dashed line, which shows there will be one zero mode for all λ_1 . Here, the extreme left Majorana mode and the extreme right Majorana mode are absent from the Hamiltonian. These modes are perfectly localised at site one and do not depend on the size of the Hamiltonian. So it can be observed for any-sized chain. The same observation can also be made from the recursion relation, where the equation becomes $\lambda_1 A_{j+1} = 0$. The equation suggests all A will be zero except A_1 , which is a free parameter, and this will turn out to be one after normalisation. See the left figure of Fig. 3.

3. $\mu = 0, \lambda_1 = 0, \lambda_2 \neq 0$

The y-axis line represents this case in the right figure of Fig. 1. There are always two zero modes in this case, except $\lambda_2 = 0$, which makes the Hamiltonian zero, so there is no real system. The parameters of this line will satisfy the relation $\lambda_2 A_{j+2} = 0$. Except for the two arbitrary coefficients, A_1 and A_2 , all coefficients must be zero. Two perfectly localised modes, one on A_1 and the other on A_2 , are shown in the middle and right figures of Fig. 3. Two sets of (A_1, A_2) that make two vectors orthogonal can also be solutions of this case, in which case they will not be separately localised, but modes will be on both sites.

4. $\mu = 0, \lambda_1 \neq 0, \lambda_2 \neq 0$

The right figure in Fig. 1 shows that there is neither a $w = 0$ region nor any region where q becomes complex. Here, $q_+ = 0$ is for all λ_1 and λ_2 irrespective of the region. The recursion relation will be $\lambda_2 A_{j+2} + \lambda_1 A_{j+1} = 0$ which suggests that A_1 is always and arbitrary coefficient. For $w = 2$ regions where $|q_-| < 1$, the solution of the recursion relation will be $A_j = \left(\frac{-\lambda_1}{\lambda_2}\right)^{j-2} A_2$. So for $w = 2$, there are two arbitrary coefficients A_1 and A_2 . That suggests if we consider the initial condition $A_2 = 0$ and $A_1 \neq 0$, then $A_j = 0$ for $j \geq 3$. This is the perfect left-edge mode. To find the other mode, A_2 must be non-zero, which in turn makes all other A_j non-zero. So, there is only one perfectly localised edge mode. One can also find both modes to be non-localised if $A_2 \neq 0$ for both modes. Here, the conditions for the localised mode depend on the initial conditions, unlike the Ising model. See the two orthogonal modes in the left and right figures of the top panel in Fig. 4 as localised and delocalised modes, respectively. In the case of $w = 1$,

$|q_-| \geq 1$, so the solution will be $A_j = 0$ for all $j \geq 2$ and $A_1 = 1$ for the normalised mode. This mode is perfectly localised at site one. If $A_2 \neq 0$, then the solution is not normalizable. Here, all the phases will have one perfectly localised mode, so there are many more points for a perfectly localised mode, unlike in the Ising case. The other mode within $w = 2$ regions is always a decreasing mode from the second site onward if $A_2 > A_1$ is chosen; otherwise, it is a decreasing mode from the first site onward. This theory has been tested experimentally, and the results are in agreement [17].

$$5. \quad \mu \neq 0, \lambda_1 \neq 0, \lambda_2 = 0$$

This is a well-known quantum Ising case where there is only one zero mode if $\lambda_1 > \mu$. The same result can be obtained from the recursion relation $\lambda_1 A_{j+1} = \mu A_j$. The solution of the equation is $A_j = \left(\frac{\mu}{\lambda_1}\right)^{j-1} A_1$. This mode will be normalizable if $\lambda_1 > \mu$, and the free coefficient A_1 can be fixed by normalisation. This case is shown by the black dotted line in Fig. 1.

$$6. \quad \mu \neq 0, \lambda_1 = 0, \lambda_2 \neq 0$$

This case is the y-axis of the left figure in Fig. 1. In Fig. 1. The number of zero modes goes from two to zero to two. The recursion relation is $\lambda_2 A_{j+2} = \mu A_j$. The two roots of the characteristic equation will be $q_{\pm} = \pm \sqrt{\frac{\mu}{\lambda_2}}$ for $\lambda_2 > 0$ and $q_{\pm} = \mp i \sqrt{\frac{\mu}{|\lambda_2|}}$ for $\lambda_2 < 0$. So the form of the general solution for both cases $A_j = [A_1 q_+^j ((-1)^{j-1} + 1) + A_2 q_+^{j-1} (1 - (-1)^{j-1})]$ is same, but q_+ will depend on sign of λ_2 . Here, for odd sites, the A_1 term will survive, and for even sites, the A_2 term. For the extreme case of initial conditions $A_1 = 0$ but $A_2 \neq 0$ or $A_1 \neq 0$ but $A_2 = 0$, the modes will have either even or odd site probabilities with a decaying envelope, as shown in the bottom panel of Fig. 4. For both non-zero A_1 and A_2 , none of the sites will reach exactly zero, but the trend will be oscillatory and decaying. The maximum probability site will be either first or second, depending on the initial choice.

$$7. \quad \mu \neq 0, \lambda_1 \neq 0, \lambda_2 \neq 0$$

This case is shown in the left figure of Fig. 1. Even though the regions G_1 and G_3 both satisfy the condition, the form of q is quite different between G_1 and G_3 . The properties of zero modes change based on parameters, even though the number of zero modes and winding numbers are constant for the whole phase.

Region G_1 : In this region λ_1, λ_2 are positive for $\mu > 0$. The general solution can be written in the following recursion form (Appendix VIF 3)

$$A_j = q_- A_{j-1} + (A_2 - q_- A_1) q_+^{j-2}$$

Since q_- and q_+ are always negative and positive, respectively, for positive values of initial conditions A_1 and A_2 , $(A_2 - q_- A_1) q_+^{j-2}$ is positive for all j . A_j will oscillate between positive and negative values depending on the relative values of q_- and $(A_2 - q_- A_1) q_+^{j-2}$. This mode can be either oscillatory decaying, or monotonically decaying, depending on parameters, as shown in Fig. 5. If the initial condition satisfies the relation $A_2 = q_- A_1$, then $A_j = q_- A_{j-1}$, the sign of A_j will change, but the probability will always decrease, $|A_j|^2 = |q_-|^2 |A_{j-1}|^2$. So, for this condition, the mode will be monotonic decay for all parameter values. The closed-form solution to the above equation will be

$$A_j = q_-^{j-2} A_2 + \sum_{k=1}^{j-2} f(k) q_-^{j-k-2}$$

where, $f(k) = (A_2 - A_1 q_-) q_+^{j-2}$.

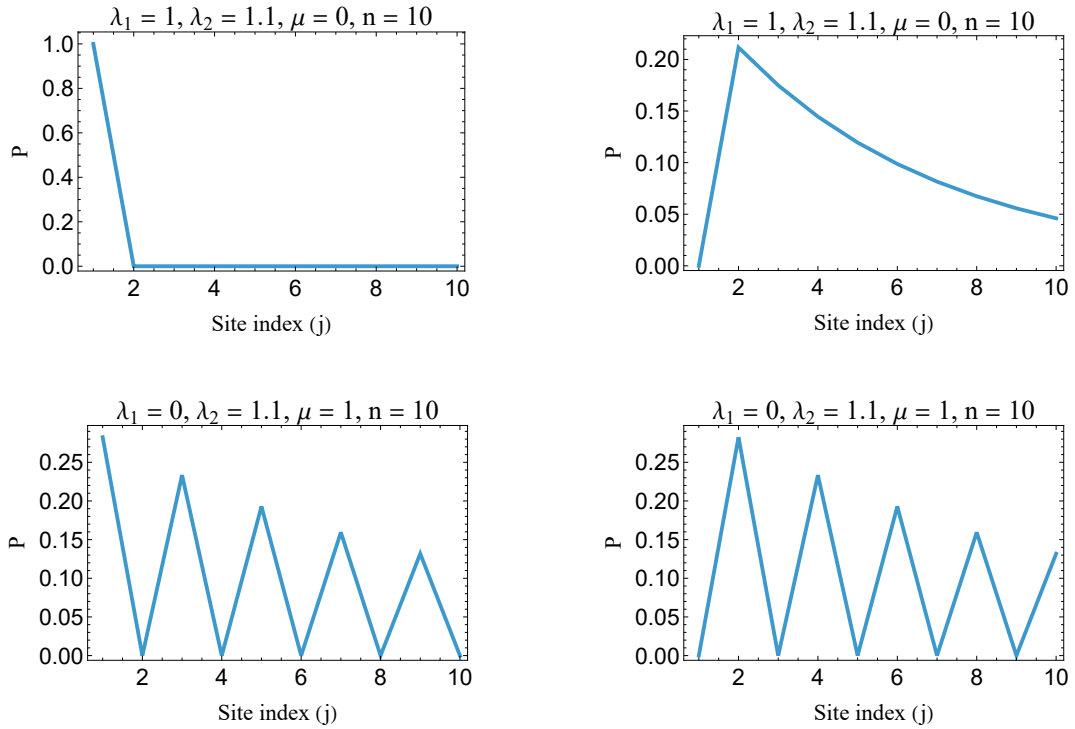


FIG. 4: (Colour online) *Top panel* is showing the probability distribution at different sites for the extended quantum Ising chain but $\mu = 0$. The left figure shows the localised mode, while the right figure shows the second delocalised mode, which is orthogonal to the first mode. *Bottom panel* is also for the extended Ising chain but $\lambda_1 = 0$. Both figures show delocalised modes in this case. The specific choice of initial conditions, $A_1 = 1$ and $A_2 = 0$ for the left figure and $A_1 = 0$ and $A_2 = 1$ for the right, ensures that the probability of alternating sites is zero.

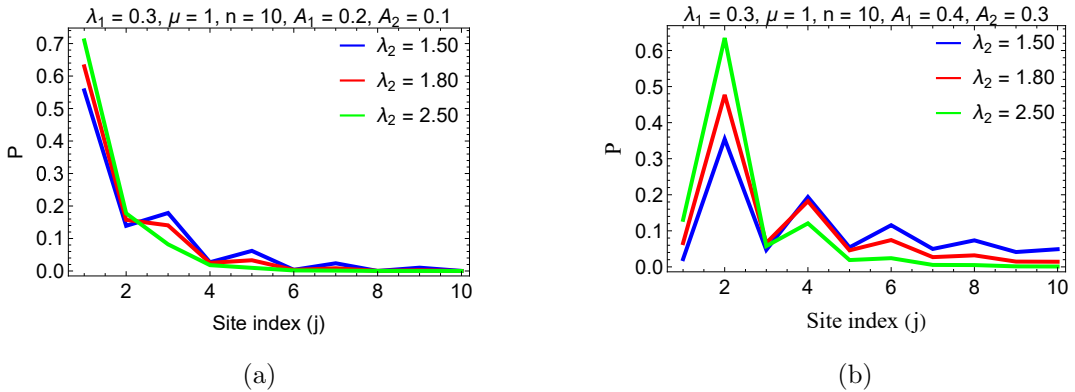


FIG. 5: (Color online) Probability distribution shows the (a) transition of oscillatory to monotonic decay mode with parameter change, (b) the corresponding orthogonal mode exhibiting oscillatory decay. The orthogonal mode corresponding to $\lambda_2 = 2.50$, which is monotonic, displays oscillatory decay. These figures suggest that in this region, both modes can be oscillatory decaying, or one mode can be oscillatory decay and the other monotonic decay.

Region G_2 : This region does not have any zero mode, even though it is a gapped region.

Region G_3 : In this region there are three types of q :

(a) Complex: The condition is $\lambda_1^2 + 4\mu\lambda_2 < 0$ and $\lambda_2 < -\mu$. The general solution can be written in the following form (Appendix VIF 1):

$$A_j = \frac{R^{j-2}}{\sin \theta} y \sin [(j-1)\theta - \phi] \quad (11)$$

where $y = \sqrt{A_1^2 R^2 + A_2^2 + 2A_1 A_2 R \cos \theta}$, $\cos \phi = \frac{A_1 R \cos \theta}{y}$, $R = \sqrt{\frac{-\mu}{\lambda_2}}$, and $\cos \theta = \frac{\lambda_1}{\sqrt{-4\mu\lambda_2}}$.

The site of maximum probability density other than first and second can be altered by varying parameters, as shown in Fig. 6. That means the zero modes can be located deep inside the bulk, but their properties will be significantly different from those of the massive bulk states. The modes can be oscillatory decaying, or monotonically decaying. In this case, to show the features, the μ is taken to be other than one, so λ_2 does not go very high. By changing μ , the area of different topological phases can be altered as shown in the right figure of Fig. 1 and Appendix.

(b) Real but equal: When $\lambda_1^2 + 4\mu\lambda_2 = 0$, both $q_+ = q_- = q$ are same then the general solution will be $A_j = (c_1 + c_2 j)r^j$ which can be written in terms of A_1 and A_2 as $A_j = [(2-j)qA_1 + (j-1)A_2]q^{j-2}$ (Appendix VIF 2).

(c) Real but different: When $\lambda_1^2 + 4\mu\lambda_2 > 0$ but $\lambda_2 < \mu - \lambda_1$ and $\lambda_2 < -\mu$. Then A_j is same as the region G_1 but with $\lambda_2 < 0$. Here, the signs of q_- and q_+ will be reversed, always remaining positive and negative, respectively. The sign of the reducing factor and additive term will be interchanged, but the explanation will remain the same.

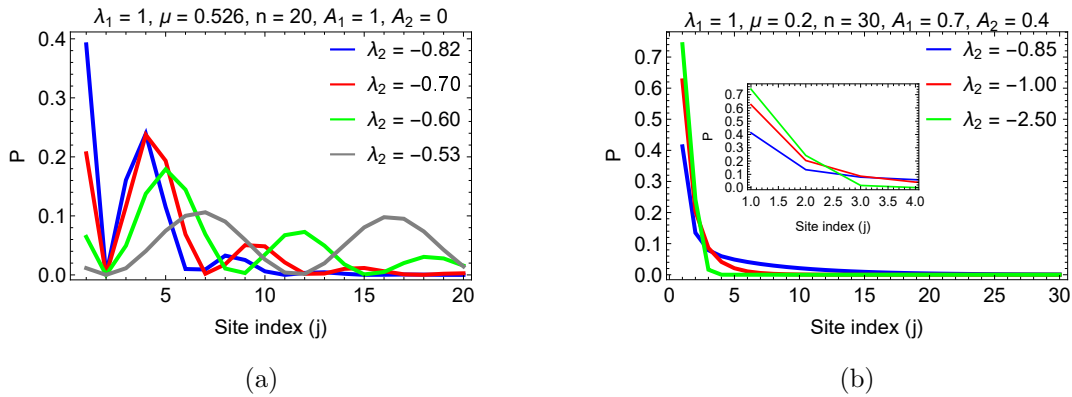


FIG. 6: (Color online) Variation of peak with parameter change (a) shows the shift of peaks for oscillatory decaying modes (b) shows purely decaying modes of different monotonicity. This indicates that this region does not always exhibit an oscillatory decaying mode, even though the q 's are complex.

Region G_4 : This region has only one normalisable q , so the general solution will be $A_j = cq_+^j$ where c will be fixed by the normalisation. The form suggests that this mode will always be monotonic decay.

IV. DIFFERENCE BETWEEN FINITE AND INFINITE SIZE MODE

The eigenmodes obtained from the recursion relation Eq. 9 do not have explicit dependence on size, and results are valid as long as the energy is zero. However, eigenenergies are shown to exhibit size dependence except when the energy is exactly zero. Since the energy depends implicitly on size, and Majorana properties are exhibited when energy is zero, the Majorana character of these modes is also influenced by the system size. Although the characteristics of zero modes are studied through the recursion relation, which is independent of size, physical systems in experimentation are inherently finite; therefore, it is necessary to compare theoretical predictions in the finite-size regime. Broadly, two cases can be distinguished: (1) one can tune the parameters such that well-approximated zero modes appear for relatively manageable sizes, and (2) when such tuning is not possible, the finite size features of the observed modes must be carefully scrutinised for potential use.

It follows from Eq. 8 that the generic eigenmodes will be linear combinations of both Majorana operators a_i and b_i . This results in overlapping modes involving both left and right edge components. The threshold for the energy to be considered zero should depend on the properties, as shown in Fig. 7. The top panel shows that when the energy is in the order of 10^{-5} , the mode is overlapping; however, the left-end probabilities are mainly from Majorana a operators, and the right end from Majorana b operators. When the size is increased, the energy decreases to the order of 10^{-12} , the mode is still overlapping, but the number of non-zero Majorana modes decreases, which suggests that the penetration length into the bulk also depends on size, as shown in the middle panel. When the mode has become perfectly left after increasing the size, the contribution of Majorana b is gone, and the energy is in the order of 10^{-15} . The threshold for the energy to be considered zero and its corresponding size are entirely parameter-dependent as shown in Fig. 8. Ideal Majorana mode features are only exhibited by perfectly localised left or right edge modes. As Fig. 7, 8 shows, energies closest to zero, although finite, still exhibit edge modes but lack Majorana character. In such cases, the recursion relation doesn't strictly hold; Instead, it satisfies the coupled relation 8, and the same features can be extracted directly from the Hamiltonian in the fermionic basis. Interestingly, the overlapping modes

approach perfectly captures left- or right-localised modes as the system size increases, eventually matching the results predicted by the recursion relation.

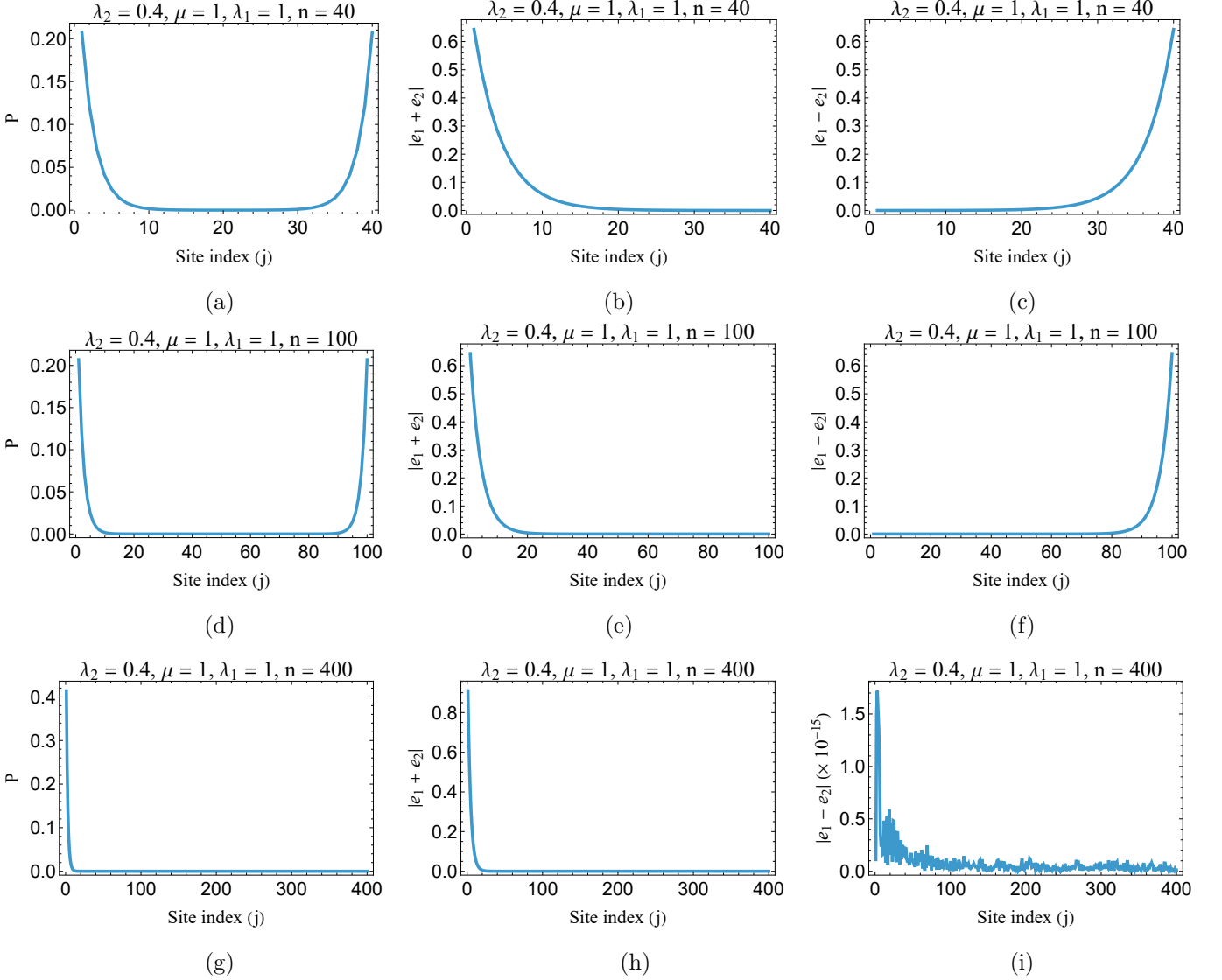


FIG. 7: (Color online) Left panels of each row show the edge modes for different sizes for $w = 1$. Their corresponding addition and difference of eigenvector plots are shown, where e_1 and e_2 are the eigenvectors ranging from 1 to n and $n + 1$ to $2n$, respectively. The former range in the eigenvector represents c , and the latter represents c^\dagger . a_i is the sum, and b_i is their difference as per the basis transformation. The eigenvalues for $n = 40$, $n = 100$ and $n = 400$ are 0.0000152638 , 1.6704×10^{-12} and 1.77636×10^{-15} , respectively, and they are closest to zero for the given parameters. It can be observed that energy decreases as size increases while keeping other parameters constant. With size, the overlapping modes collapse into either left or right edge mode, and this happens when the coefficients of a_i are zero throughout the lattice sites and the coefficients of b_i keep decreasing from left to right.

The size and energy associated with it will depend on the parameters, whether it should be considered zero or not because it can still give rise to overlapping modes with Majorana or non-Majorana properties, even when the energy is considerably small, as seen in Fig. 8. The properties of the modes also vary with size; for example, a mode can transition from an oscillatory decaying mode to a decaying mode or vice versa. The energy modes unaffected by size are those that directly go out of the Hamiltonian based on some parameters, and those are the same as those found from the recursion relation or directly from the Hamiltonian of any size.

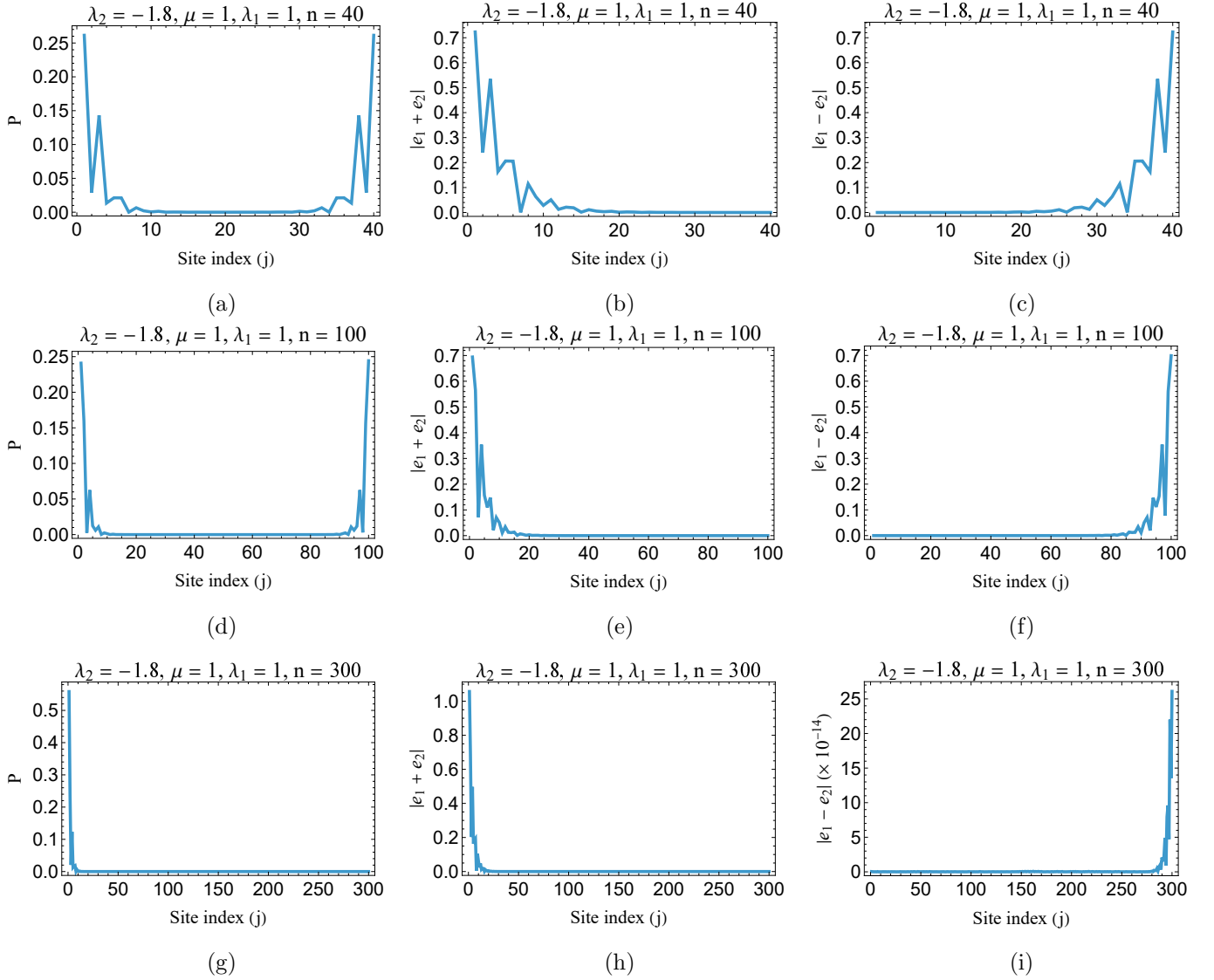


FIG. 8: (Color online) Left panels of each row show the edge modes for different sizes for the bottom $w = 2$ region. Their corresponding addition and difference of eigenvectors are shown in the middle and right panels. The eigenvalue for $n = 40$, $n = 100$ and $n = 300$ are 8.65056×10^{-6} , -1.60729×10^{-13} and 8.51156×10^{-16} respectively. A similar trend to Fig. 7 can be observed where either one of a_i or b_i approaches zero as size increases and the overlapping modes collapse to either left or right edges.

V. DISCUSSION

The winding number, or the number of zero modes, remains constant for a particular phase and changes only at the phase transition. But the nature of the zero modes varies even within the same phase. That happens because parameters can change without affecting the phase. This change of parameters varies the roots of the characteristic equation continuously. The number of normalizable modes is determined by the modulus of q , which must be less than one. We demonstrated that the roots can also determine the phase transition. It can help determine how far the phase transition is. This can also help choose the appropriate-sized chain for perfect left or right modes, as close to one $|q|$ will have a larger penetration depth, which would require a bigger size of chain to avoid overlap. This helps in choosing the parameters that do not change the phase by a slight variation in the parameters.

Since the recursion relation yields the perfect Majorana zero modes, this analysis enables us to characterise the modes in different regimes, independent of size. The perfect localised zero modes are also possible in the three-spin interaction Hamiltonian, and the parameter space required to achieve these is bigger, unlike in the Ising model,

where there is only one point for a zero chemical potential. It is also shown that out of two zero modes, one can be perfectly localised or both, depending on the parameters and initial conditions of the two probability amplitudes. We also demonstrated that if these zero modes are not perfectly localised, then they need not have to be the highest probability near the extreme ends of the chain; rather, they can be tuned to any other site, even deep within the bulk. This raises an important point: the Majorana zero modes can also lie in the bulk. However, this is only possible when the q are complex or equal. But these bulk modes have very different properties from the massive bulk modes, as they exhibit a decaying tail on either side, unlike other bulk modes. For the finite-size chain, none of these properties are consistent except for the perfectly localised modes until the appropriate size is chosen so that the energy is well approximated to be zero. Until a proper size is selected, the modes will overlap in the amplitudes of the left and right sites. The size also depends on parameters. So, in the finite case, every property needs to be checked separately because its size dependence is different. Even if the size is small, the mode with the least absolute energy in the spectrum still exhibits a decaying tail into the bulk, a feature characteristic of zero modes, without satisfying the Majorana properties. In conclusion, the zero modes, edge modes, and Majorana zero modes can be identical for a given parameter, but their dependence on size is distinct.

ACKNOWLEDGMENTS

VP would like to thank Professor R.Srikanth for the financial assistance through the Indian Science and Engineering Research Board (SERB) grant CRG/2022/008345. SS would like to thank CRG/2021/000996.

-
- [1] R. Moessner and J. E. Moore, *Topological Phases of Matter* (Cambridge University Press, 2021).
[2] T. D. Stanescu, *Introduction to topological quantum matter & quantum computation* (CRC Press, 2024).
[3] R. M. Lutchyn, E. P. Bakkers, L. P. Kouwenhoven, P. Krogstrup, C. M. Marcus, and Y. Oreg, *Nature Reviews Materials* **3**, 52 (2018).
[4] L. Fu and C. Kane, in *APS March Meeting Abstracts* (2008) pp. V10–001.
[5] C. W. J. Beenakker, *Annual Review of Condensed Matter Physics* **4**, 113 (2013).
[6] D. Aasen, M. Hell, R. V. Mishmash, A. Higginbotham, J. Danon, M. Leijnse, T. S. Jespersen, J. A. Folk, C. M. Marcus, K. Flensberg, *et al.*, *Physical Review X* **6**, 031016 (2016).
[7] A. Y. Kitaev, *Physics-Uspekhi* **44**, 131 (2001).
[8] M. H. Freedman, A. Kitaev, M. J. Larsen, and Z. Wang, *Annals of Physics* **303**, 2 (2003).
[9] Y. Niu, S. B. Chung, C.-H. Hsu, I. Mandal, S. Raghu, and S. Chakravarty, *Physical Review B* **85** (2012), 10.1103/physrevb.85.035110.
[10] A. Alecce and L. Dell’Anna, *Physical Review B* **95** (2017), 10.1103/physrevb.95.195160.
[11] A. Kopp and S. Chakravarty, *Nature Physics* **1**, 53 (2005).
[12] S. Rahul, R. R. Kumar, Y. Kartik, and S. Sarkar, *Journal of the Physical Society of Japan* **90**, 094706 (2021).
[13] S. Sarkar, *Scientific reports* **8**, 5864 (2018).
[14] I. Mahyaeh and E. Ardonne, *Journal of Physics Communications* **2**, 045010 (2018).
[15] O. Viyuela, D. Vodola, G. Pupillo, and M. A. Martin-Delgado, *Physical Review B* **94** (2016), 10.1103/physrevb.94.125121.
[16] Y. Nambu, *Physical Review* **117**, 648 (1960).
[17] S. L. D. ten Haaf, Y. Zhang, Q. Wang, A. Bordin, C.-X. Liu, I. Kulesh, V. P. M. Sietses, C. G. Prosko, D. Xiao, C. Thomas, M. J. Manfra, M. Wimmer, and S. Goswami, *Nature* **641**, 890 (2025).

VI. APPENDIX

A. Critical lines and points

To find out those points, we need to set the ground state energy to zero, which is possible only if $\chi_y(k)$ and $\chi_z(k)$ shown in Eq. 3 are both simultaneously zero. $\chi_y(k)$ will be zero for $k = 0, \pm\pi$ and $k = \cos^{-1}\left(\frac{-\lambda_1}{2\lambda_2}\right)$. If for these points $\chi_z(k)$ is also equal to zero, then these k-points will be phase transition points.

- For $k = 0$, $\chi_z(k) = -2\lambda_1 - 2\lambda_2 + 2\mu$. This implies that gap closing points ($\chi_z(k) = 0$) will be for $\lambda_1 + \lambda_2 = \mu$ line. See Fig. 1(C_2)
- For $k = \pm\pi$, $\chi_z(k) = 2\lambda_1 - 2\lambda_2 + 2\mu$. This implies that gap closing points ($\chi_z(k) = 0$) will be for $\lambda_2 - \lambda_1 = \mu$ line. See Fig. 1(C_1)

- For $k = \cos^{-1}\left(\frac{-\lambda_1}{2\lambda_2}\right)$, $\chi_z(k) = 2\lambda_2 + 2\mu$. This implies that gap closing points ($\chi_z(k) = 0$) will be for $\lambda_2 + \mu = 0$ line but $\lambda_1 \leq 2\lambda_2$ to make argument of cosine less than one. See Fig. 1(C_3)
- Multi critical point M_1 will have zeros for $k = 0, \pm\pi$ but M_2 will be zero only for $k = 0$ since k value for zero energy change for critical line C_3 with λ_1 and λ_2 . See Fig. 1

B. Majorana basis transformation

To convert the equation

$$H = -\mu \sum_{j=1}^N (1 - 2c_j^\dagger c_j) - \lambda_1 \sum_{j=1}^{N-1} (c_j^\dagger c_{j+1} + c_j^\dagger c_{j+1}^\dagger + c_{j+1}^\dagger c_j + c_{j+1} c_j) - \lambda_2 \sum_{j=2}^{N-1} (c_{j-1}^\dagger c_{j+1} + c_{j+1}^\dagger c_{j-1}^\dagger + c_{j+1}^\dagger c_{j-1} + c_{j-1} c_{j+1}) \quad (12)$$

into the Majorana basis, we use the normalised conversion such that the eigenvalues exactly match in both bases $a_i = \frac{c_i + c_i^\dagger}{\sqrt{2}}$, $b_i = \frac{-i(c_i^\dagger - c_i)}{\sqrt{2}}$, Such that $a_j^2 = b_j^2 = \frac{1}{2}$, $\{a_i, b_j\} = 0$, and $\{a_i, a_j\} = \{b_i, b_j\} = \delta_{i,j}$.

We can write after the inverse transformation $c_i = \frac{1}{\sqrt{2}}(a_i - ib_i)$ $c_i^\dagger = \frac{1}{\sqrt{2}}(a_i + ib_i)$.

In both bases, the constant terms are not removed from the Hamiltonian; rather, they are automatically absorbed. The μ term

$$H = -\mu \sum_{j=1}^N (1 - 2c_j^\dagger c_j) = -\mu \sum_{j=1}^N (c_j c_j^\dagger - c_j^\dagger c_j) = -\mu \sum_{j=1}^N ((a_j - ib_j)(a_j + ib_j) - (a_j + ib_j)(a_j - ib_j))$$

After changing the bases

$$H = -\frac{\mu}{2} \sum_{j=1}^N ((a_j - ib_j)(a_j + ib_j) - (a_j + ib_j)(a_j - ib_j)) = -i\mu \sum_{j=1}^N (a_j b_j - b_j a_j)$$

For the other two terms, substituting in Eq. 12 and using the anti-commutation properties, terms like $a_i a_j$ and $a_j a_i$ cancel out, the same applies for $b_i b_j$ and $b_j b_i$ as well.

$$H = -i\mu \sum_{j=1}^N (a_j b_j - b_j a_j) - i\lambda_1 \sum_{j=1}^{N-1} (b_j a_{j+1} - a_{j+1} b_j) - i\lambda_2 \sum_{j=2}^{N-1} (b_{j-1} a_{j+1} - a_{j+1} b_{j-1})$$

$$H = -2i \left[-\mu \sum_{j=1}^N b_j a_j + \lambda_1 \sum_{j=1}^{N-1} b_j a_{j+1} + \lambda_2 \sum_{j=2}^{N-1} b_{j-1} a_{j+1} \right]$$

C. Recursion relation and its solution

$$H = -i \begin{pmatrix} 0 & \mu & 0 & \cdots & & \\ -\mu & 0 & \lambda_1 & 0 & \lambda_2 & \cdots \\ 0 & -\lambda_1 & 0 & \mu & 0 & \cdots \\ 0 & 0 & -\mu & 0 & \lambda_1 & 0 \\ \vdots & \vdots & \vdots & \ddots & \ddots & \ddots \end{pmatrix}.$$

If the general eigenvector has the form $\psi = (A_1, A'_1, A_2, A'_2, \dots, A_N, A'_N)^T$ then the eigenvalue equation will be $H\psi = E\psi$ and that will lead to two equations, one from odd rows and other from even

$$-\mu A_j + \lambda_1 A_{j+1} + \lambda_2 A_{j+2} = iE A'_j \quad (13a)$$

$$\mu A'_j - \lambda_1 A'_{j-1} - \lambda_2 A'_{j-2} = iE A_j \quad (13b)$$

The first equation will have terms like A_{N+1} and A_{N+2} for $j = N$ but those sites are not present in the chain so $A_{N+1} = 0 = A_{N+2}$. Similarly, the second equation will have absent sites terms from chain like A_{-1} and A_{-2} , so $A_{-1} = 0 = A_{-2}$.

D. Number of zero modes

Let us assume λ_1 and μ are positive.

- Region G_1 : $\lambda_2 > \mu + \lambda_1$. In this case both $|q_{\pm}| < 1$, two normalisable modes.
- Line C_1 : $\lambda_2 = \mu + \lambda_1$. then $q_+ = \frac{\mu}{\mu + \lambda_1}$ and $q_- = -1$, only one normalisable mode.
- Region G_4 : $\mu - \lambda_1 < \lambda_2 < \mu + \lambda_1$. Here, $|q_+| < 1$ but $|q_-| > 1$, only one normalisable mode.
- Point M_1 : $\lambda_1 = 0$ and $\lambda_2 = \mu$, $q_{\pm} = \frac{|\mu|}{\mu}$. So both $|q_{\pm}| = 1$, no normalisable modes.
- Region G_2 : $\lambda_2 < \mu - \lambda_1$ but greater than $-\mu$. Both $|q_{\pm}| > 1$, no normalisable modes.
- Line C_2 : $\lambda_2 = \mu - \lambda_1$, Here, there are three cases: (a) If $\lambda_1 < 2\mu$ then $|q_+| = 1$ and $|q_-| > 1$, no normalisable mode. (b) If $\lambda_1 > 2\mu$ then $|q_+| < 1$ and $|q_-| = 1$, one normalisable mode (c) If $\lambda_1 = 2\mu$ which is Point M_2 , then both $|q_{\pm}| = 1$, no normalisable mode.
- Line C_3 : $\lambda_2 = -\mu$. Here there are two cases: (a) If $\lambda_1 < 2\mu$ then the term within the square root becomes negative, so q_{\pm} become complex, but their modulus will always be one, no normalizable mode; (b) If $\lambda_1 > 2\mu$ then q_{\pm} will remain real but only $|q_+|$ will be less than one so only one normalizable mode.
- Region G_3 : $\lambda_2 < \mu - \lambda_1$ but less than $-\mu$. Here, both $|q_{\pm}| < 1$, so there are two normalizable modes.
- Dashed curve in Fig. 1 shows the parameters for $q_+ = q_-$. Both q below the dashed curve will be complex but distinct with $|q_+| = |q_-|$. Above the curve will have real q .

E. General solution for $w = 2$

The recursion relation will have two normalizable roots in the $w = 2$ regions. The general solution of amplitude at the j -th site can be written in terms of arbitrary coefficients as

$$A_j = c_1 q_+^j + c_2 q_-^j$$

This equation can be converted into two physically realizable terms: $A_1 = c_1 q_+ + c_2 q_-$ and $A_2 = c_2 q_+^2 + c_1 q_-^2$. After solving $c_1 = \frac{A_1 q_- - A_2}{q_+ (q_- - q_+)}$ and $c_2 = \frac{A_1 q_+ - A_2}{q_- (q_+ - q_-)}$ in terms of A_1 and A_2 , the general solution will be

$$A_j = \frac{1}{q_+ - q_-} [A_1 (q_+ q_-^{j-1} - q_- q_+^{j-1}) + A_2 (q_+^{j-1} - q_-^{j-1})]$$

F. General solution in the region G_3

$$1. \quad \lambda_1^2 + 4\mu\lambda_2 < 0 \text{ and } \lambda_2 < -\mu$$

The roots q_{\pm} are complex and can be written as $q_{\pm} = R e^{\pm i\theta}$ where $R = \sqrt{\frac{\mu}{\lambda_2}}$ and $\theta = \frac{\lambda_1}{\sqrt{-4\mu\lambda_2}}$. The terms in the general solution will be $(q_+ q_-^{j-1} - q_- q_+^{j-1}) = 2iR^j \sin(j-2)\theta$, $(q_+^{j-1} - q_-^{j-1}) = 2iR^{j-1} \sin(j-1)\theta$, and $q_+ - q_- = 2iR \sin \theta$. After using $\sin(j-2)\theta = \sin(j-1)\theta \cos \theta - \cos(j-1)\theta \sin \theta$, the solution can be written as $A_j = \frac{R^{j-2}}{\sin \theta} [(A_1 R \cos \theta + A_2) \sin(j-1)\theta - A_1 R \sin \theta \cos(j-1)\theta]$. After defining $y = \sqrt{(A_1 R \cos \theta + A_2)^2 + (A_1 R \sin \theta)^2}$ and $\cos \phi = \frac{A_1 R \cos \theta + A_2}{y}$,

$$A_j = \frac{R^{j-2}}{\sin \theta} y \sin [(j-1)\theta - \phi]$$

$$2. \quad \lambda_1^2 + 4\mu\lambda_2 = 0 \text{ and } \lambda_2 < -\mu$$

The dashed curve in Fig. 1 will have both q values the same, $q_+ = q = q_-$. The general solution will be $A_j = (c_1 + c_2j)q^j$ where $A_1 = (c_1 + c_2)q$ and $A_2 = (c_1 + 2c_2)q^2$. After replacing the $c_1 = \frac{2A_1q - A_2}{q^2}$ and $c_2 = \frac{A_2 - A_1q}{q^2}$ in terms of A_1 and A_2 ,

$$A_j = [(2-j)qA_1 + (j-1)A_2]q^{j-2}$$

$$3. \quad \lambda_1^2 + 4\mu\lambda_2 > 0, \lambda_2 < -\mu, \text{ and } \lambda_2 < \mu - \lambda_1$$

Within this condition, both q 's will be real and $|q| < 1$. The terms $q_+^j - q_-^j = (q_+ - q_-)q_+^{j-1} + q_-(q_+^{j-1} - q_-^{j-1})$ can be changed in the general solution $A_j = \frac{1}{q_+ - q_-} [-A_1q_+q_-(q_+^{j-2} - q_-^{j-2}) + A_2(q_+^{j-1} - q_-^{j-1})]$, the new A_j will be

$$A_j = \frac{1}{q_+ - q_-} [-A_1q_+q_-(q_+^{j-3} + q_-(q_+^{j-3} - q_-^{j-3})) + A_2((q_+ - q_-)q_+^{j-2} + q_-(q_+^{j-2} - q_-^{j-2}))]$$

After rearranging,

$$A_j = \frac{q_-}{q_+ - q_-} [-A_1q_+q_-(q_+^{j-3} - q_-^{j-3}) + A_2(q_+^{j-2} - q_-^{j-2})] + q_+^{j-2} [-A_1q_- + A_2]$$

$$A_j = q_-A_{j-1} + (A_2 - q_-A_1)q_+^{j-2}$$

The solution of the above equation is

$$A_j = q_-^{j-2}A_2 + \sum_{k=1}^{j-2} f(k)q_-^{j-k-2}$$

where, $f(k) = (A_2 - A_1q_-)q_+^{j-2}$